

Optimal pair density functional for description of nuclei with large neutron excess

M. Yamagami,^{1,2} Y. R. Shimizu,³ and T. Nakatsukasa²

¹*Department of Computer Science and Engineering,*

University of Aizu, Aizu-Wakamatsu, Fukushima 965-8580, Japan

²*RIKEN Nishina Center, RIKEN, Hirosawa 2-1, Wako, Saitama 351-0198, Japan*

³*Department of Physics, Kyushu University, Fukuoka 812-8581, Japan*

(Dated: November 11, 2018)

Toward a universal description of pairing properties in nuclei far from stability, we extend the energy density functional by enriching the isovector density dependence in the particle-particle channel (pair density functional, pair-DF). We emphasize the necessity of both the linear and quadratic isovector density terms. The parameters are optimized by the Hartree-Fock-Bogoliubov calculation for 156 nuclei of the mass number $A = 118 - 196$ and the asymmetry parameter $(N - Z)/A < 0.25$. We clarify that the pair-DF should include the isovector density dependence in order to take into account the effect of the isoscalar and isovector effective masses in the particle-hole channel consistently. The different Skyrme forces can give the small difference in the pairing gaps toward the neutron drip line, if the optimal pair-DF consistent with the particle-hole channel is employed.

PACS numbers: 21.10.Re, 21.60.Ev, 21.60.Jz

I. INTRODUCTION

The energy density functional (EDF) theory provides a comprehensive microscopic framework for description of bulk nuclear properties, low-lying excitations, giant vibrations, and rotational excitations [1]. From the pioneering work by Vautherin and Brink [2], diverse endeavors have been made for finding the best EDF aiming at the description of the nuclear properties across the mass table. For example, the Skyrme functional for the particle-hole (p-h) channel has been improved by taking into account the incompressibility modulus of nuclear matter [3], the spin- and spin-isospin channels [4], the deformation properties [5], the spin-orbit terms [6], and the isospin properties [7]. Efforts to include the new terms such as the tensor terms are also being made (for the recent situation, see Ref. [8]).

The particle-particle (p-p) channel of the EDF (pair density functional, pair-DF) is also an indispensable element for description of nuclear systems [9]. The study of the nuclear matter predicts a very weak 1S_0 pairing at the normal density, and the pairing correlation in finite nuclei is considered to be nuclear surface effects [10]. The induced pairing interaction due to phonon exchange also enhances the surface effect [10, 11, 12]. These facts suggest the density dependence of the effective pairing force.

The standard parametrization of the pair-DF has the isoscalar density ($\rho = \rho_n + \rho_p$) dependence only [13, 14, 15, 16, 17]. The coupling constant should be constrained by the requirement to reproduce the experimental data such as masses, low-lying excited states, and rotational properties. However, the functional form of the density dependence is still under discussion [9, 18].

In nuclei near the β -stability line, the effect of the p-h field characterized by the Fermi energy is much stronger than the p-p field. Therefore the pairing correlations can be treated within the BCS approximation [9, 19].

On the other hand, the strengths for the p-p and p-h channels become comparable in magnitude for weakly-bound nuclei [9, 19, 20, 21, 22, 23, 24]. Therefore it is desirable to constrain the functional form of the pair-DF by using the experimental data of unstable nuclei.

The isovector density ($\rho_1 = \rho_n - \rho_p$) dependence can have sizable effects in nuclei apart from the β -stability line. In Ref. [25], the linear ρ_1 terms were introduced so as to simulate the neutron pairing gaps in symmetric and neutron matters obtained with either the bare interaction or the interaction screened by the medium polarization effects. It was pointed out that the pairing properties in semi-magic nuclei can be better described by the ρ_1 -dependent pair-DF than that without ρ_1 terms [26].

We also recognized the importance of the linear ρ_1 term in the pair-DF [24]. By performing the Hartree-Fock-Bogoliubov (HFB) calculation with various coupling constants of the ρ and ρ_1 terms, we emphasized the strong sensitivity to the pairing properties and the influence on rotational excitations in deformed nuclei near the neutron drip line.

In principle, it is desirable to derive the pair-DF from the bare interaction based on the microscopic pairing theory including both the medium polarization effect and the surface phonon coupling effect in finite nuclei. However, it seems very difficult at present in spite of recent progress toward this direction [12, 27, 28, 29, 30, 31, 32, 33, 34, 35].

In this paper, we extend the pair-DF by including the linear and *quadratic* ρ_1 terms based on the phenomenological considerations. The pair-DF is designed so as to reproduce the dependence of pairing gaps on both the mass number A and the asymmetry parameter $\alpha = (N - Z)/A$. The parameters in the pair-DF are optimized so as to minimize the root-mean-square (r.m.s.) deviation between the experimental and calculated pairing gaps. The necessity of the ρ_1 dependence in pair-DF is emphasized in connection with the the effective mass

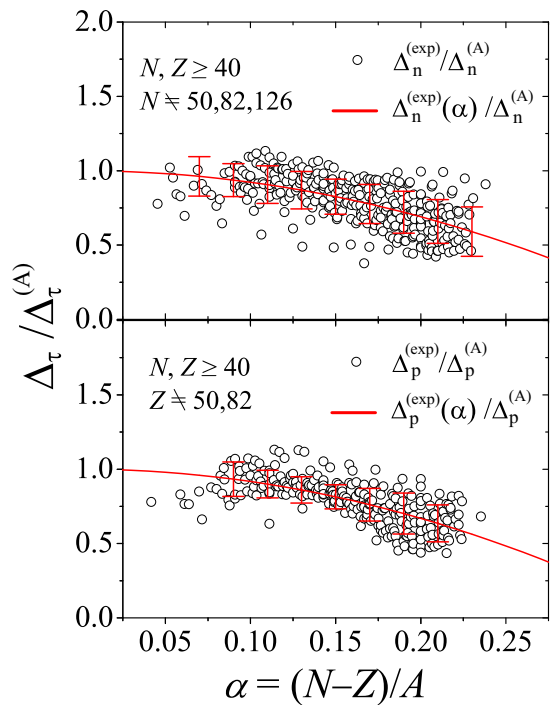


FIG. 1: (Color online) Experimental neutron pairing gaps (upper panel) and those of proton (lower panel) in the region of $N, Z \geq 40$ (except for nuclei with either $Z = 50, 82$, or $N = 50, 82, 126$) are shown as a function of α . The pairing gaps are divided by $\Delta_\tau^{(A)}$. The error bar represents the r.m.s. deviation from the average trend $\Delta_\tau^{(\text{exp})}(\alpha)$ for each α with $\Delta\alpha = 0.02$ interval.

parameters.

This paper is organized as follows. In Sec.II, we briefly review the global properties of pairing gaps. In Sec.III, our pair-DF including the linear and quadratic ρ_1 terms is introduced. In Sec. IV, we point out the drawback of the pair-DF without the ρ_1 terms. In Sec. V and VI, we investigate the role of the ρ_1 terms. The parameters in the pair-DF are determined by the HFB calculation for 156 nuclei of $A = 118 - 196$ and $\alpha < 0.25$. We clarify the close connection between the pair-DF and the effective masses by the extensive analysis with 13 Skyrme parameters. The choice of the pairing strength is discussed in Sec. VII. The conclusion is drawn in Sec. VIII.

II. GLOBAL TREND OF PAIRING GAPS

We construct the pair-DF so as to reproduce the A - and α -dependence of pairing gaps. In Ref.[36], Vogel *et al.* pointed out that the experimental pairing gaps in the region of $50 < Z < 82$ and $82 < N < 126$ can be well parametrized by $\Delta(\alpha) = (1 - 6.1\alpha^2)\Delta^{(A)}$. Here the A dependent part is given by $\Delta^{(A)} = 7.2/A^{1/3}$ MeV. This average A - and α -dependence holds for both neutron and proton pairing gaps.

We extend the analysis with up-to-date measured masses in the wider mass region of $N, Z \geq 40$ (except for nuclei with either $Z = 50, 82$ or $N = 50, 82, 126$) [37]. The result is shown in Fig. 1. The average A - and α -dependence is determined for the neutron and proton pairing gaps separately by χ^2 -fitting;

$$\begin{aligned} \Delta_n^{(\text{exp})}(\alpha)/\Delta_n^{(A)} &\equiv C_{n,\text{exp}}^{(0)} - C_{n,\text{exp}}^{(1)}\alpha^2 \\ &= 1 - 7.74\alpha^2, \end{aligned} \quad (1)$$

$$\begin{aligned} \Delta_p^{(\text{exp})}(\alpha)/\Delta_p^{(A)} &\equiv C_{p,\text{exp}}^{(0)} - C_{p,\text{exp}}^{(1)}\alpha^2 \\ &= 1 - 8.25\alpha^2, \end{aligned} \quad (2)$$

with $\Delta_n^{(A)} = 6.75/A^{1/3}$ MeV and $\Delta_p^{(A)} = 6.36/A^{1/3}$ MeV. Here the experimental pairing gaps are extracted by the odd-even mass difference with the three-point staggering parameters [18].

The Coulomb force is an important building block of nuclear systems. The 20 - 30 % reduction of Δ_p by the self-consistent treatment of the Coulomb force was reported in Ref. [38]. The authors of Ref. [39] also arrived at the same conclusion by performing the HFB calculation with the non-empirical pair-DF. On the other hand, the experimental evidence is unclear in our analysis. The ratio is $\Delta_p^{(\text{exp})}(\alpha)/\Delta_n^{(\text{exp})}(\alpha) \approx 0.94(1 - 0.51\alpha^2) \geq 0.91$ for $0 \leq \alpha \leq 0.25$. This is smaller than the uncertainty of our analysis about 10 % shown by error bars in Fig. 1. The elaborate investigation is required to clarify the Coulomb effect. Therefore we neglect this effect in our analysis and leave it as an open problem in the future study.

III. MODEL

A. Parametrization of pair-DF

We extend the pair-DF by including the linear and quadratic ρ_1 terms in the following form;

$$H_{\text{pair}}(\mathbf{r}) = \frac{V_0}{4} \sum_{\tau=n,p} g_\tau[\rho, \rho_1] \{\tilde{\rho}_\tau(\mathbf{r})\}^2 \quad (3)$$

with

$$g_\tau[\rho, \rho_1] = 1 - \eta_0 \frac{\rho(\mathbf{r})}{\rho_0} - \eta_1 \frac{\tau_3 \rho_1(\mathbf{r})}{\rho_0} - \eta_2 \left(\frac{\rho_1(\mathbf{r})}{\rho_0} \right)^2. \quad (4)$$

Here $\tau = n$ (neutron) or p (proton), and $\rho_0 = 0.16 \text{ fm}^{-3}$ is the saturation density of symmetric nuclear matter. The $\tau_3 = 1$ (n) or -1 (p) in the linear ρ_1 term is introduced so as to preserve the charge symmetry of the pair-DF. In nuclei with large α , the ρ_1 terms produce two effect for pairing correlations. The one is the volume effect inside the nucleus, which is relevant to all nuclei. The other is the skin effect in nuclei apart from the β -stability line.

The pair-DF with $\eta_0 = 0.5$ and $\eta_1 = \eta_2 = 0$ is one of the current standard parameterizations called the mixed-type pairing force. This pairing force reproduces the average A dependence of pairing gaps [18]. We also justify

this choice in Sec. V. Therefore, we fix $\eta_0 = 0.5$ unless otherwise noted.

B. Setup

We use the standard Skyrme interaction for the p-h channel in the HFB calculation. The Skyrme SLy4 [7] parametrization is mainly used. In Sec. VI, we will extend our analysis with 13 Skyrme parameters.

For the determination of η_1 and η_2 , we perform the Skyrme-HFB calculation for 156 ground states of even-even, open-shell nuclei in the region of $Z = 56 - 76$, and either $N = 56 - 76$ or $88 - 120$, which covers the range of $0 < \alpha < 0.25$. We utilize the computer code of the Skyrme-HFB calculation developed by M. Stoitsov *et al.* [40]. Starting from the spherical, prolate and oblate initial conditions, the lowest energy solution is searched in the space of axially symmetric quadrupole deformation.

We estimate the r.m.s. deviations between the experimental and calculated pairing gaps in order to optimize the η_1 and η_2 . The neutron and proton r.m.s. deviations are defined by

$$\sigma_\tau = \left[\frac{1}{N_\tau^{(\text{exp})}} \sum_{\text{all data}} \left(\Delta_\tau - \Delta_\tau^{(\text{exp})} \right)^2 \right]^{1/2}. \quad (5)$$

The total r.m.s. deviation is also given by

$$\sigma_{\text{tot}} = \left[\frac{N_n^{(\text{exp})} \sigma_n^2 + N_p^{(\text{exp})} \sigma_p^2}{N_n^{(\text{exp})} + N_p^{(\text{exp})}} \right]^{1/2}. \quad (6)$$

Here $N_\tau^{(\text{exp})}$ is the number of existing data of $\Delta_\tau^{(\text{exp})}$ in the region of the present investigation; $N_n^{(\text{exp})} = 93$ and $N_p^{(\text{exp})} = 84$. The theoretical pairing gap is defined by [41, 42, 43]

$$\Delta_\tau = - \int d\mathbf{r} \tilde{\rho}_\tau(\mathbf{r}) \tilde{h}_\tau(\mathbf{r}) / \int d\mathbf{r} \tilde{\rho}_\tau(\mathbf{r}), \quad (7)$$

when the local pairing potential is given by

$$\tilde{h}_\tau(\mathbf{r}) = \frac{\partial}{\partial \tilde{\rho}_\tau(\mathbf{r})} \int d\mathbf{r}' H_{\text{pair}}(\mathbf{r}'). \quad (8)$$

We extract the coefficients $C_\tau^{(i)}$ which represent the average α -dependence of pairing gaps,

$$\Delta_\tau(\alpha) = \left(C_\tau^{(0)} - C_\tau^{(1)} \alpha^2 \right) \Delta_\tau^{(A)}, \quad (9)$$

by χ^2 -fitting analysis for Δ_τ of the 156 nuclei. Here $\Delta_\tau^{(A)}$ is the same quantity determined for Eqs.(1) and (2).

For each set of (η_0, η_1, η_2) , the strength V_0 is fixed so as to reproduce the $\Delta_n^{(\text{exp})}$ of ^{156}Dy . We use the abbreviation $V_0[\Delta_n(^{156}\text{Dy})]$ for this choice. This nucleus has quadrupole deformation $\beta \approx 0.28$ [44]. The experimental

| E_{cut} | $V_0[\Delta_n(^{156}\text{Dy})]$ | σ_{tot} | σ_n | σ_p | $C_n^{(0)}$ | $C_n^{(1)}$ | $C_p^{(0)}$ | $C_p^{(1)}$ |
|------------------|----------------------------------|-----------------------|------------|------------|-------------|-------------|-------------|-------------|
| 50 | -346.5 | 0.17 | 0.16 | 0.17 | 1.08 | 9.42 | 1.00 | 8.13 |
| 75 | -320.0 | 0.17 | 0.16 | 0.18 | 1.07 | 9.26 | 1.01 | 8.44 |

TABLE I: The cutoff quasiparticle energy E_{cut} dependence of the r.m.s. deviations [MeV] and the coefficients $C_\tau^{(i)}$ are listed. The parameters $(\eta_0, \eta_1, \eta_2) = (0.5, 0.2, 2.5)$ are fixed. The strength V_0 [MeV fm $^{-3}$] is constrained by the $\Delta_n^{(\text{exp})}$ of ^{156}Dy .

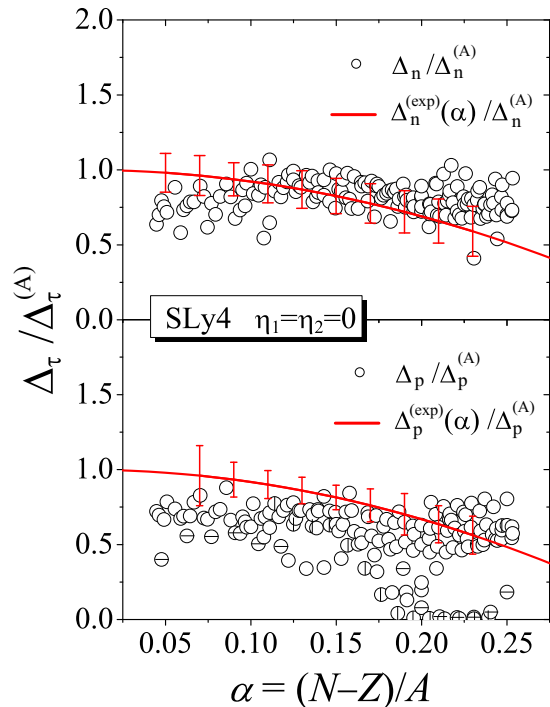


FIG. 2: (Color online) Neutron and proton pairing gaps obtained with $\eta_0 = 0.5$ and $\eta_1 = \eta_2 = 0$ are plotted as a function of α . The pairing gaps are divided by $\Delta_\tau^{(A)}$. The ^{60}Nd and ^{70}Yb isotopes possessing the large proton shell gaps are indicated by circles with horizontal and vertical bars respectively in the bottom panel.

pairing gaps are $\Delta_n^{(\text{exp})} = 1.17$ MeV and $\Delta_p^{(\text{exp})} = 0.98$ MeV, which are close to $\Delta_n^{(\text{exp})}(\alpha) = 1.04$ MeV and $\Delta_p^{(\text{exp})}(\alpha) = 0.96$ MeV estimated by Eqs.(1) and (2). The justification of V_0 will be discussed in Sec. VII.

The cutoff quasiparticle energy $E_{\text{cut}} = 50$ MeV is fixed in this paper. We checked the dependence of σ_τ and $C_\tau^{(i)}$ on the E_{cut} in Table I. The results with $E_{\text{cut}} = 50$ and 75 MeV agree within a few percent accuracy. Here the parameters of the pair DF are fixed to be $(\eta_0, \eta_1, \eta_2) = (0.5, 0.2, 2.5)$, which are the optimal choice (See Sec. V).

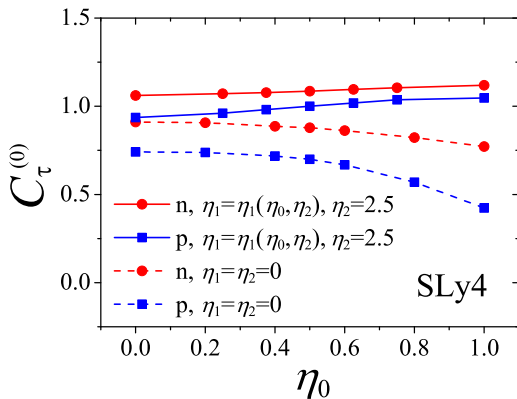


FIG. 3: (Color online) The coefficient $C_\tau^{(0)}$ obtained with $\eta_1 = \eta_2 = 0$ is shown as a function of η_0 . The result with $\eta_2 = 2.5$ and $\eta_1(\eta_0, \eta_2)$ is compared. Here $\eta_1(\eta_0, \eta_2)$ is the value of η_1 minimizing σ_{tot} for each (η_0, η_2) with $V_0[\Delta_n(^{156}\text{Dy})]$.

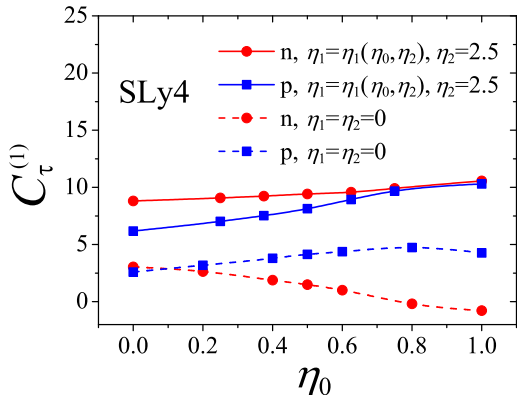


FIG. 4: (Color online) The same with Fig. 3 but for the coefficient $C_\tau^{(1)}$.

IV. PAIR-DF WITHOUT ρ_1 TERM

We show the drawback of the pair-DF without the ρ_1 terms. The pairing gaps obtained with $\eta_0 = 0.5$, $\eta_1 = \eta_2 = 0$, and the strength $V_0[\Delta_n(^{156}\text{Dy})] = -324.0$ MeV fm $^{-3}$ are plotted in Fig. 2. The extracted $C_\tau^{(0)}$ and $C_\tau^{(1)}$ are shown by the dashed lines in Figs. 3 and 4. The Δ_n and Δ_p are almost α -independent. The coefficient $C_n^{(1)} = 1.11$ is much smaller than the experimental value $C_{n,\text{exp}}^{(1)} = 7.74$. Although the $C_p^{(1)} = 3.74$ is larger than $C_n^{(1)} = 1.11$, this is due to the collapse of the pairing gap in weak pairing region. Actually, it would be $C_p^{(1)} = 1.38$, if we restrict the data to $\Delta_p > 0.25$ MeV. Here the ^{60}Nd and ^{70}Yb isotopes possessing the large proton shell gaps are indicated by circles with horizontal and vertical bars respectively in the bottom panel of Fig. 2. The collapse of Δ_p is a drawback of the mean-field approximation [45], and can be overcome by performing the particle number projection (PNP). The improvement

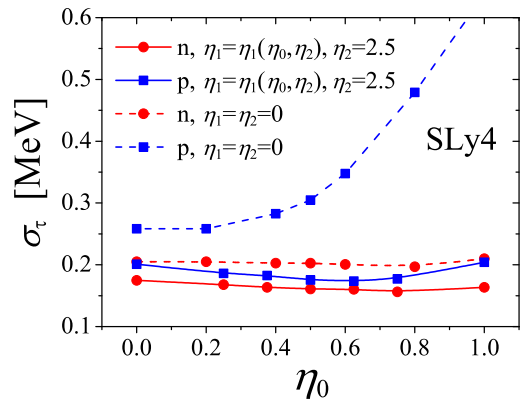


FIG. 5: (Color online) The same with Fig. 3 but for σ_τ .

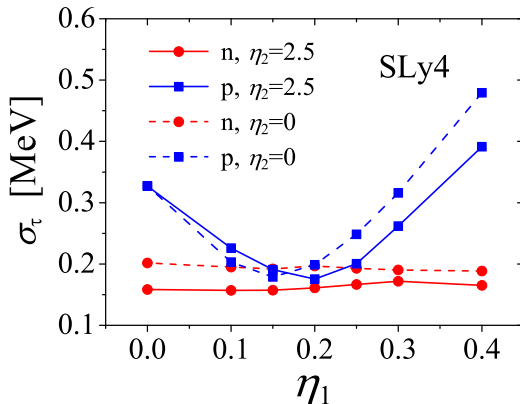


FIG. 6: (Color online) The r.m.s. deviations are shown as a function of η_1 . The results with either $\eta_2 = 0$ or 2.5 are compared.

for the $C_\tau^{(1)}$ values, however, can not be expected by the PNP procedure [46], because the PNP method does not have any specific isovector effect. Therefore, we neglect the effect of PNP in this study.

The $C_n^{(0)} = 0.84$ is smaller than $C_{n,\text{exp}}^{(0)} = 1$. The $C_p^{(0)} = 0.67$ is smaller than $C_n^{(0)}$ due to the quenching of Δ_p attributed to the neutron skin effect [24]: The neutron skin reduces the overlap between the form factor $[1 - \eta_0 \rho(\mathbf{r})/\rho_0]$ and $\tilde{\rho}_p(\mathbf{r})$ in Eq.(3).

The quenching of Δ_p due to the neutron skin effect becomes stronger with larger η_0 [24]. The σ_τ is shown as a function of η_0 by the dashed line in Fig. 5. Because the σ_p rapidly increases with η_0 , the minimum of σ_{tot} is absent. In addition, the $C_\tau^{(0)}$ and $C_\tau^{(1)}$ remain small if restricted to $\eta_1 = \eta_2 = 0$ (See Figs. 3 and 4).

V. ROLE OF ρ_1 DEPENDENCE

It is possible to compensate the quenching of Δ_p by using a stronger pairing strength for proton (for example, Ref. [48, 55, 56]). However it violates the charge symme-

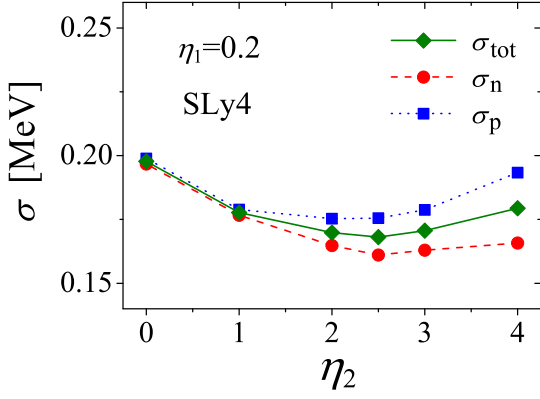


FIG. 7: (Color online) The r.m.s deviations at $\eta_1 = 0.2$ are shown as a function of η_2 .

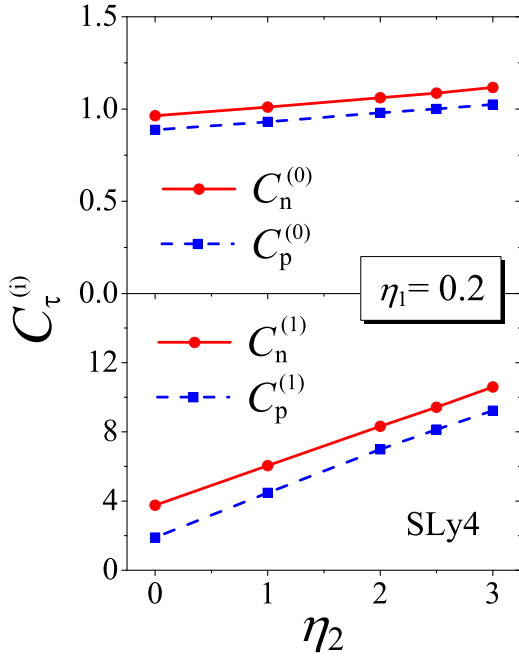


FIG. 8: (Color online) The coefficients $C_\tau^{(i)}$ at $\eta_1 = 0.2$ are shown as a function of η_2 .

try of the pair-DF. This is the important symmetry in the theoretical framework, and indispensable for global description of pairing properties from neutron to proton drip line.

This consideration leads to introduction of the linear ρ_1 term in Eq. (4). This pair-DF preserves the charge symmetry. The ρ_1 term induces the difference of the neutron and proton pairing strengths automatically [24]. The σ_p has the minimum value at $\eta_1 = 0.15$, while the σ_n is almost constant as a function of η_1 . This is shown by the dashed lines in Fig. 6. We obtain the $C_n^{(0)} = 0.93$ and $C_p^{(0)} = 0.83$ with $\eta_1 = 0.15$ and $\eta_2 = 0$, which are better than those with $\eta_1 = \eta_2 = 0$. However, the $C_n^{(1)} = 3.75$ and $C_p^{(1)} = 1.89$ at $\eta_1 = 0.15$ do not improve as a function

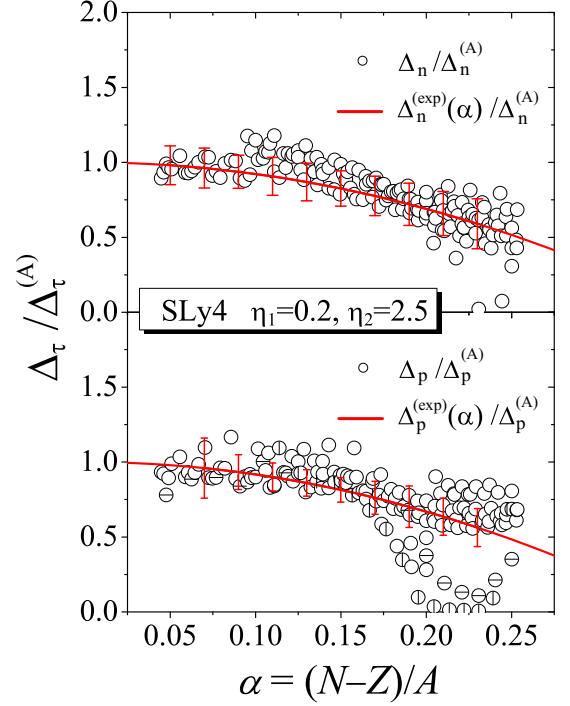


FIG. 9: (Color online) The same as Fig. 2 but with $(\eta_0, \eta_1, \eta_2) = (0.5, 0.2, 2.5)$.

| criteria | V_0 | σ_{tot} | σ_n | σ_p | $C_n^{(0)}$ | $C_n^{(1)}$ | $C_p^{(0)}$ | $C_p^{(1)}$ |
|----------------------------------|--------|-----------------------|------------|------------|-------------|-------------|-------------|-------------|
| $V_{\text{opt}}(\text{def})$ | -344.0 | 0.16 | 0.14 | 0.18 | 1.03 | 9.71 | 0.99 | 7.64 |
| $V_{\text{opt}}(\text{sph})$ | -308.0 | 0.50 | 0.47 | 0.52 | 0.59 | 6.23 | 0.52 | 4.62 |
| $V_0[\Delta_n(^{156}\text{Dy})]$ | -346.5 | 0.17 | 0.16 | 0.17 | 1.08 | 9.42 | 1.00 | 8.13 |
| $V_0[\Delta_n(^{120}\text{Sn})]$ | -322.0 | 0.34 | 0.30 | 0.37 | 0.76 | 7.87 | 0.69 | 6.11 |
| Exp | - | - | - | - | 1.00 | 7.74 | 1.00 | 8.25 |

TABLE II: The r.m.s. deviations and the coefficients $C_\tau^{(i)}$ obtained with the SLy4 force and the optimal parameters $(\eta_0, \eta_1, \eta_2) = (0.5, 0.2, 2.5)$ are shown. The results with $V_{\text{opt}}(\text{def})$, $V_{\text{opt}}(\text{sph})$, $V_0[\Delta_n(^{156}\text{Dy})]$, and $V_0[\Delta_n(^{120}\text{Sn})]$ are compared. The experimental values of $C_\tau^{(i)}$ are also listed.

of η_1 .

The quadratic ρ_1 term in the pair-DF improves the r.m.s. deviations. To see this, the r.m.s. deviations are plotted as a function of η_1 while keeping $\eta_2 = 2.5$ in Fig. 6. Those with $\eta_1 = 0.2$ are plotted as a function of η_2 in Fig. 7. The parameter set of $(\eta_1, \eta_2) = (0.2, 2.5)$ simultaneously gives the minimum values of σ_{tot} , σ_n and σ_p . They are smaller than those at $\eta_2 = 0$

The quadratic ρ_1 term also improves the α -dependence. The $C_\tau^{(0)}$ and $C_\tau^{(1)}$ at $\eta_1 = 0.2$ are plotted as a function of η_2 in Fig. 8. The $C_\tau^{(0)}$ stays around 1.0, while the $C_\tau^{(1)}$ increases linearly and reaches $C_\tau^{(1)} \approx C_{\tau, \text{exp}}^{(1)} \approx 8$ at $\eta_2 = 2.5$.

The pairing gaps obtained with $(\eta_1, \eta_2) = (0.2, 2.5)$ are shown in Fig. 9. The r.m.s. deviations and the coef-

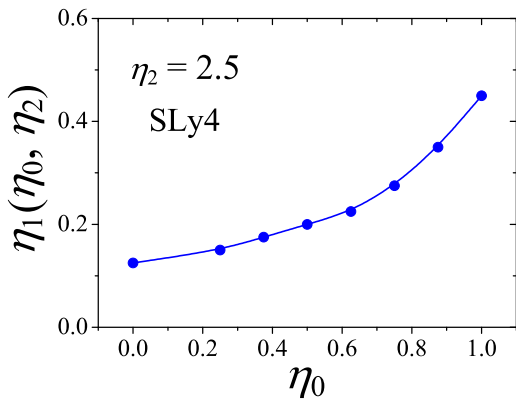


FIG. 10: (Color online) The value of η_1 minimizing the σ_{tot} for each (η_0, η_2) with $V_0[\Delta_n(^{156}\text{Dy})]$ is plotted as a function of η_0 . The $\eta_2 = 2.5$ is fixed.

ficients $C_\tau^{(i)}$ are listed in Table II. We see the significant improvement compared to those with $\eta_1 = \eta_2 = 0$.

The optimized set of (η_1, η_2) gives the justification of the mixed type pairing force ($\eta_0 = 0.5$). The σ_τ with $\eta_2 = 2.5$ and $\eta_1(\eta_0, \eta_2)$ is shown as a function of η_0 by the solid line in Fig. 5. The improvement over the choice $\eta_1 = \eta_2 = 0$, especially the large reduction of σ_p , is obvious. Therefore, the minimum of σ_{tot} can appear at $\eta_0 \approx 0.5$. Here $\eta_1(\eta_0, \eta_2)$ is the value of η_1 minimizing σ_{tot} for each (η_0, η_2) with $V_0[\Delta_n(^{156}\text{Dy})]$. The $\eta_1(\eta_0, \eta_2)$ at $\eta_2 = 2.5$ is shown as a function of η_0 in Fig. 10.

The coefficients $C_\tau^{(0)}$ and $C_\tau^{(1)}$ with $\eta_2 = 2.5$ and $\eta_1(\eta_0, \eta_2)$ are shown as a function of η_0 by the solid lines in Fig. 3 and 4. The $C_\tau^{(0)}$ is insensitive to η_0 , while the $C_\tau^{(1)}$ becomes close to the experimental value at $\eta_0 \approx 0.5$.

VI. EFFECTIVE MASS AND ρ_1 -DEPENDENCE OF PAIR-DF

A. Isoscalar and isovector effective masses

Pairing correlations are sensitive to the single-particle structure around the Fermi level. For a suggestive example, the pairing gap is a function of gG and given by $\Delta \propto e^{-1/gG}$ for $gG \ll 1$ in the schematic model of the seniority pairing force with the strength G and the uniform single-particle level density g [45]. On the other hand, the effective mass has a strong influence on the single-particle energies. The average level density is proportional to the effective mass [10]. Therefore, we expect the close connection between the effective mass and the pair-DF in order to reproduce the global trend of the experimental pairing gaps.

For the investigation, we extend our analysis with 13 Skyrme parameterizations; SkM* [5], SGII [4], LNS [47], SkP [19], BSk17 [48], SkT6 [49], SLy4, SLy5 [7], SkI1, SkI3, SkI4 [6], SkO, and SkO' [50].

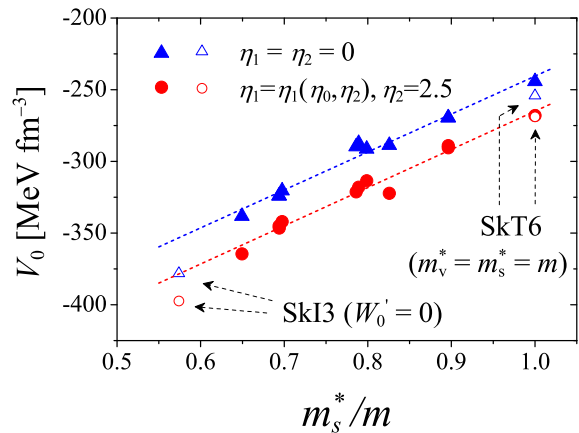


FIG. 11: (Color online) The strength V_0 reproducing the $\Delta_n^{(\text{exp})}$ of ^{156}Dy for each Skyrme force is plotted in relation to m_s^*/m . The results with $\eta_2 = 2.5$ and the optimal η_1 in Table III are compared to those with $\eta_1 = \eta_2 = 0$. The $\eta_0 = 0.5$ is fixed.

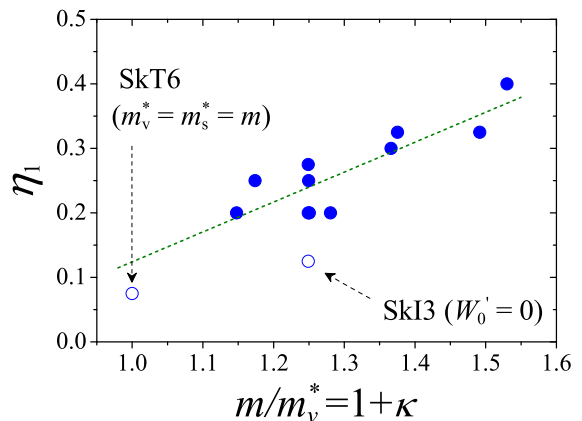


FIG. 12: (Color online) The optimal value of η_1 minimizing σ_{tot} with $(\eta_0, \eta_2) = (0.5, 2.5)$ and $V_0[\Delta_n(^{156}\text{Dy})]$ is shown in relation to m/m_v^* . See text for details.

The effective mass of the Skyrme force is given by

$$\frac{\hbar^2}{2m_\tau^*(\mathbf{r})} = \frac{\hbar^2}{2m} + b_1\rho - b'_1\rho_\tau \quad (10)$$

$$= \frac{\hbar^2}{2m} \left\{ \frac{m}{m_s^*} + \tau_3 I \Delta m_1 \right\} \quad (11)$$

with $I(\mathbf{r}) = \rho_1/\rho$ and $\Delta m_1(\mathbf{r}) = m/m_s^* - m/m_v^*$ [1, 58]. The isoscalar and isovector effective masses are defined by

$$\frac{m}{m_s^*(\mathbf{r})} = 1 + \frac{2m}{\hbar^2} \left(b_1 - \frac{b'_1}{2} \right) \rho \quad (12)$$

$$\frac{m}{m_v^*(\mathbf{r})} = 1 + \frac{2m}{\hbar^2} b_1 \rho = 1 + \kappa. \quad (13)$$

The m_v^* is directly connected to the enhancement factor κ of the Thomas-Reiche-Kuhn sum rule [51]. We esti-

| Skyrme | m_v^*/m | m_s^*/m | Δm_1 | W'_0/W_0 | η_J | η_1 | $V_0[\Delta_n(^{156}\text{Dy})]$ | σ_{tot} | σ_n | σ_p | $C_n^{(0)}$ | $C_n^{(1)}$ | $C_p^{(0)}$ | $C_p^{(1)}$ |
|--------|-----------|-----------|--------------|------------|----------|----------|----------------------------------|-----------------------|------------|------------|-------------|-------------|-------------|-------------|
| SkM* | 0.653 | 0.788 | -0.262 | 1 | 0 | 0.400 | -318.0 | 0.15 | 0.13 | 0.16 | 1.09 | 9.84 | 0.97 | 7.86 |
| SGII | 0.670 | 0.786 | -0.219 | 1 | 0 | 0.325 | -321.3 | 0.15 | 0.15 | 0.16 | 1.09 | 9.38 | 0.95 | 8.10 |
| LNS | 0.727 | 0.825 | -0.164 | 1 | 0 | 0.325 | -322.2 | 0.17 | 0.13 | 0.21 | 1.09 | 11.58 | 0.98 | 8.95 |
| SkP | 0.732 | 1.000 | -0.366 | 1 | 1 | 0.300 | -268.0 | 0.16 | 0.19 | 0.12 | 1.07 | 9.05 | 0.92 | 8.24 |
| Bsk17 | 0.780 | 0.798 | -0.028 | 1 | 1 | 0.200 | -313.5 | 0.14 | 0.14 | 0.13 | 1.08 | 8.68 | 0.94 | 6.94 |
| SLy4 | 0.800 | 0.694 | 0.190 | 1 | 0 | 0.200 | -346.5 | 0.17 | 0.16 | 0.17 | 1.08 | 9.42 | 1.00 | 8.13 |
| SLy5 | 0.800 | 0.697 | 0.184 | 1 | 1 | 0.200 | -342.0 | 0.16 | 0.15 | 0.16 | 1.06 | 8.94 | 0.98 | 8.38 |
| SkI1 | 0.800 | 0.693 | 0.191 | 1 | 0 | 0.250 | -345.0 | 0.18 | 0.15 | 0.20 | 0.97 | 4.62 | 0.96 | 6.16 |
| SkI4 | 0.800 | 0.649 | 0.290 | -0.985 | 0 | 0.275 | -364.5 | 0.18 | 0.16 | 0.20 | 1.02 | 8.25 | 0.97 | 7.57 |
| SkO | 0.851 | 0.896 | -0.058 | -1.125 | 0 | 0.250 | -290.5 | 0.17 | 0.18 | 0.17 | 1.05 | 6.91 | 0.91 | 6.24 |
| SkO' | 0.871 | 0.896 | -0.032 | -0.576 | 1 | 0.200 | -289.0 | 0.16 | 0.16 | 0.15 | 1.03 | 6.62 | 0.89 | 5.64 |
| SkI3 | 0.800 | 0.574 | 0.493 | 0 | 0 | 0.125 | -397.4 | 0.20 | 0.20 | 0.20 | 1.04 | 7.26 | 0.98 | 8.63 |
| SkT6 | 1.000 | 1.000 | 0.000 | 1 | 1 | 0.075 | -268.9 | 0.17 | 0.21 | 0.11 | 1.11 | 7.93 | 0.92 | 6.97 |

TABLE III: The parameter set of the optimal pair-DF for each Skyrme parameterization is listed. The optimal value of η_1 minimizing σ_{tot} with the strength $V_0[\Delta_n(^{156}\text{Dy})]$ [MeV fm⁻³], the r.m.s. deviations [MeV], and the coefficients $C_\tau^{(i)}$ are shown. The parameters $(\eta_0, \eta_2) = (0.5, 2.5)$ are fixed for them. The effective masses m_v^* and m_s^* at the saturation density of symmetric nuclear matter, the difference $\Delta m_1 = m/m_s^* - m/m_v^*$, and the W'_0/W_0 and η_J of the spin-orbit potential are also listed.

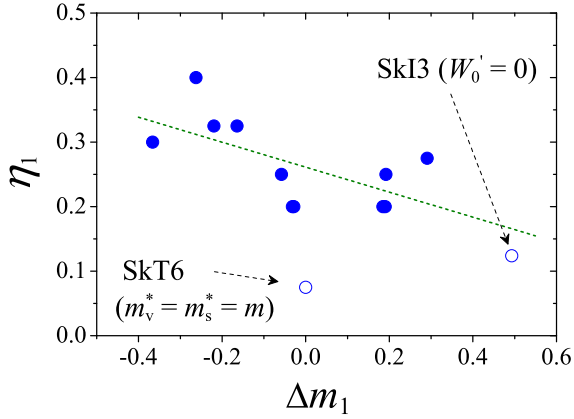


FIG. 13: (Color online) The same with Fig. 12 but in relation to Δm_1 .

mate the m_s^* and m_v^* at the saturation density of the symmetric nuclear matter. The m_v^* is a key parameter which determines the splitting of the neutron and proton effective masses as a function of I . The parameters b_1 and b'_1 [50] are given by

$$b_1 = \frac{1}{8} [t_1 (2 + x_1) + t_2 (2 + x_2)] \quad (14)$$

$$b'_1 = \frac{1}{8} [t_1 (1 + 2x_1) - t_2 (1 + 2x_2)]. \quad (15)$$

The spin-orbit potential $\mathbf{W}_\tau(\mathbf{r})$ also has the ρ_1 dependence. The $\mathbf{W}_\tau(\mathbf{r})$ of Skyrme DF is defined by

$$\begin{aligned} \mathbf{W}_\tau(\mathbf{r}) &= \frac{1}{2} (W_0 \nabla \rho + W'_0 \nabla \rho_\tau) + \eta_J \mathbf{W}_\tau^J \\ &= \left(\frac{W_0}{2} + \frac{W'_0}{4} \right) \nabla \rho + \tau_3 \frac{W'_0}{4} \nabla \rho_1 + \eta_J \mathbf{W}_\tau^J \end{aligned}$$

where $\mathbf{W}_\tau^J(\mathbf{r}) = C_0^J \mathbf{J} + \tau_3 C_1^J \mathbf{J}_1$ with the parameter η_J of either 0 or 1. The \mathbf{J} (\mathbf{J}_1) is the isoscalar (isovector) spin-current density. The C_0^J and C_1^J are given by t_1 , t_2 , x_1 and x_2 of the Skyrme parameter [52]. Most Skyrme functionals have the spin-orbit terms with $W_0 = W'_0$. However, the SkI4, SkO, and SkO' have the generalized ρ_1 dependence by introducing the different strengths W_0 and W'_0 . The SkI3 has $W'_0 = 0$.

We search the optimal value of η_1 which minimizes σ_{tot} under the conditions; 1) the fixed $(\eta_0, \eta_2) = (0.5, 2.5)$, and 2) the strength V_0 reproducing the $\Delta_n^{(\text{exp})}$ of ^{156}Dy . The numerical uncertainty is $\delta\eta_1 = 0.025$. The results are summarized in Table III.

The strengths V_0 reproducing the $\Delta_n^{(\text{exp})}$ of ^{156}Dy are plotted in relation to m_s^*/m in Fig. 11. For $\eta_1 = \eta_2 = 0$, the V_0 increases linearly. This trend is in agree with the general consideration that the pairing strength should be increased if the level density is low. The relation is given by $V_0 = -505.05 + 264.47 m_s^*/m$ MeV fm⁻³ with the correlation coefficient $r = 0.99$, except for SkT6 and SkI3 (See Appendix A for the procedure of the correlation analysis). In general, the linear correlation disappears with the ρ_1 terms due to the η_1 and η_2 dependence of V_0 . However, it is interesting to mention that the linear correlation is recovered with $\eta_2 = 2.5$ and the optimal η_1 . The extracted correlation is $V_0 = -531.45 + 266.46 m_s^*/m$ MeV fm⁻³ with $r = 0.99$.

The optimal values of η_1 are shown in relation to m/m_v^* in Fig. 12. The linear correlation between η_1 and m/m_v^* is obvious, irrespective of the choice of W'_0 and η_J . The extracted relation is given by

$$\eta_1 = -0.340 + 0.464 \frac{m}{m_v^*}, \quad (16)$$

or, in terms of the enhancement factor

$$\eta_1 = 0.124 + 0.464 \kappa, \quad (17)$$

except for SkI3 and SkT6. The correlation coefficient between η_1 and m/m_v^* is $r = 0.85$. This indicates that these parameters is almost linearly dependent. The possible reason for the deviation of SkI3 and SkT6 is the special assumption on the Skyrme DF. The SkT6 sets $m_s^* = m_v^* = m$ by definition. The SkI3 neglects the ρ_1 term in the spin-orbit potential by setting $W_0' = 0$.

During the optimization of the pair-DF, the $\eta_2 = 2.5$ for SLy4 is used for other Skyrme parameters to avoid the huge computational task. However, the improvement obtained by the optimization of the parameter η_2 should be small. The effect can be estimated as follows: We define the r.m.s. deviation of $C^{(1)}$ by

$$\Delta C^{(1)} = \sqrt{\langle (C_\tau^{(1)} - C_{\tau,\text{exp}}^{(1)})^2 \rangle}. \quad (18)$$

Here $C_{\tau,\text{exp}}^{(1)}$ is the experimental value of Eqs. (1) and (2). The $\Delta C^{(1)} = 1.5$ is obtained by taking the average $\langle \rangle$ over $\tau = n, p$ and the 13 Skyrme parameters. If the linearity $\Delta\eta_2 \approx \Delta C^{(1)}/2.3$ of Fig. 8 and the parabolic approximation for σ_{tot} as a function of η_2 from Fig. 7 are assumed for the other Skyrme parameters, the expected improvement for σ_{tot} is about 0.002 MeV. In addition, we will show that the difference in the pairing gaps for different Skyrme forces is small if the pair-DF with $\eta_2 = 2.5$ and the optimal η_1 is used in Sec. VII.

From the present analysis, we conclude that the pair-DF should include the ρ_1 dependence in order to take into account the effect of the m_s^* and m_v^* for the global description of pairing correlations.

B. Δm_1 dependence

The effective masses m_s^* and m_v^* have strong correlation with the V_0 and η_1 of the pair DF respectively. On the other hand, the splitting of neutron and proton effective masses directly depends on the local asymmetry parameter $I(\mathbf{r})$ through the combination of m_s^* and m_v^* ; $\Delta m_1 = m/m_s^* - m/m_v^*$. If Δm_1 is negative, the m_p^* (m_n^*) is a decreasing (increasing) function of I . In order to compensate the effect, the larger η_1 is necessary so as reproduce the same magnitude of the $\Delta_p^{(\text{exp})}(\alpha)$ and $\Delta_n^{(\text{exp})}(\alpha)$ (See Eqs. (1) and (2)). On the other hand, the smaller η_1 is required for the positive Δm_1 .

This correlation can be seen in Fig. 13. The extracted correlation is

$$\eta_1 = 0.261 - 0.193\Delta m_1 \quad (19)$$

with $r = -0.63$, except for SkT6 and SkI3. Although this correlation is weaker than that between η_1 and m/m_v^* due to the scattering of the m_s^*/m value, it is meaningful to conclude the linear dependence between η_1 and Δm_1 . The $\eta_1 \approx 0.26$ at $\Delta m_1 \approx 0$ can be the rough estimation of the η_1 compensating the artificial Δ_p suppression due to the neutron skin effect.

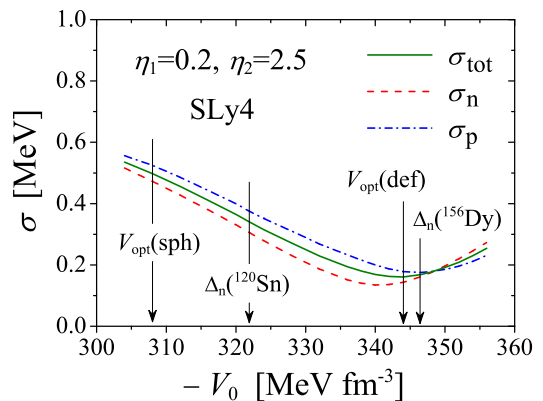


FIG. 14: (Color online) The r.m.s. deviations with SLy4 force and $(\eta_0, \eta_1, \eta_2) = (0.5, 0.2, 2.5)$ are shown as a function of V_0 . The strengths $V_{\text{opt}}(\text{def})$, $V_{\text{opt}}(\text{sph})$, $V_0[\Delta_n(^{156}\text{Dy})]$, and $V_0[\Delta_n(^{120}\text{Sn})]$ are indicated by arrows.

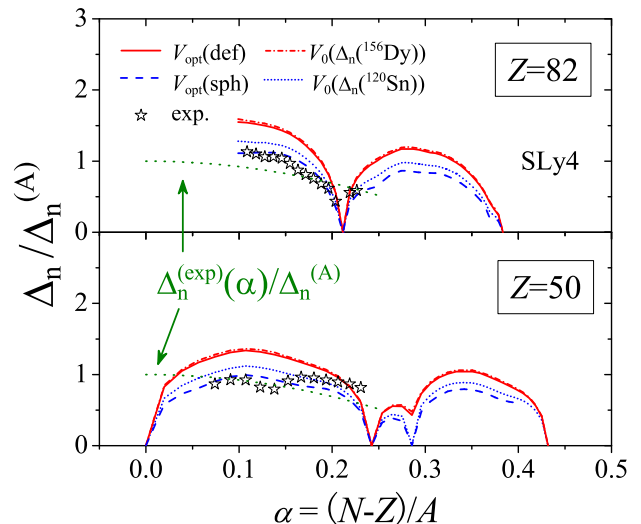


FIG. 15: (Color online) The neutron pairing gap of Sn and Pb isotopes with SLy4 force and $(\eta_0, \eta_1, \eta_2) = (0.5, 0.2, 2.5)$ are shown as a function of α . The results with the strengths; $V_{\text{opt}}(\text{def})$, $V_{\text{opt}}(\text{sph})$, $V_0[\Delta_n(^{156}\text{Dy})]$, and $V_0[\Delta_n(^{120}\text{Sn})]$ are compared. The experimental trend $\Delta_n^{(\text{exp})}(\alpha)$ is shown up to $\alpha < 0.25$ together with the experimental data.

VII. CHOICE OF V_0

It is desirable to optimize the strength V_0 for experimental data in wide region of nuclear chart. However, the procedure demands heavy computational efforts. Therefore the V_0 is usually fixed so as to reproduce a pairing gap of specific nucleus. Several authors adopted the $\Delta_n^{(\text{exp})}$ of ^{120}Sn [46, 53, 54]. The strength $V_0[\Delta_n(^{120}\text{Sn})] = -322.0 \text{ MeV fm}^{-3}$ with SLy4 force and $(\eta_1, \eta_2) = (0.2, 2.5)$ gives $\sigma_{\text{tot}} = 0.34 \text{ MeV}$ (see Table. II). On the other hand, if the V_0 is fixed in deformed region, for example, $V_0[\Delta_n(^{156}\text{Dy})] = -346.5 \text{ MeV fm}^{-3}$

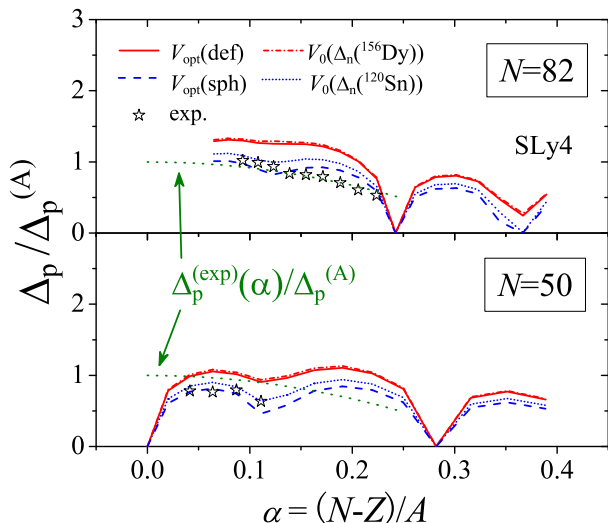


FIG. 16: (Color online) The same with Fig. 15 but for the proton pairing gaps of $N = 50$ and 82 isotones.

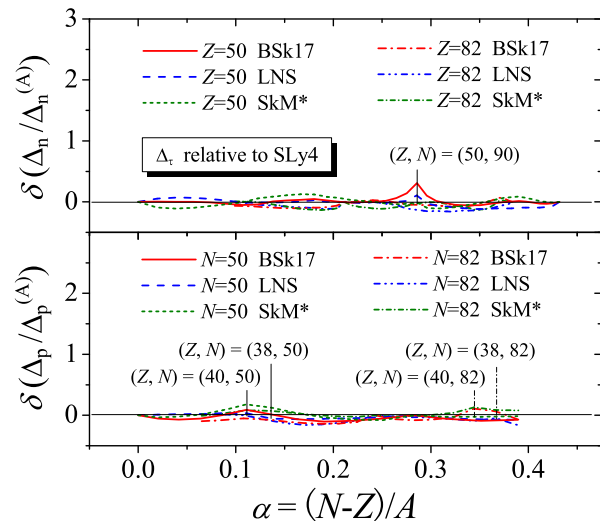


FIG. 17: (Color online) The difference in the pairing gaps for the different Skyrme parameters. See text for details.

the r.m.s. deviation reduces to $\sigma_{\text{tot}} = 0.17$ MeV. The V_0 dependence of the σ_{tot} is shown in Fig. 14. The optimal value $V_{\text{opt}}(\text{def}) = -344.0$ MeV fm $^{-3}$ for the deformed nuclei is close to the $V_0[\Delta_n(^{156}\text{Dy})]$.

In Figs. 15 and 16, the Δ_n of Sn and Pb isotopes and the Δ_p of $N = 50$ and 82 isotones obtained with SLy4 force and $(\eta_1, \eta_2) = (0.2, 2.5)$ are shown. The results with $V_{\text{opt}}(\text{def})$, $V_0[\Delta_n(^{156}\text{Dy})]$, $V_0[\Delta_n(^{120}\text{Sn})]$ are compared. The difference of the results with $V_{\text{opt}}(\text{def})$ and $V_0[\Delta_n(^{156}\text{Dy})]$ is negligible along the isotopic and isotonic chains. However, the choice of $V_0[\Delta_n(^{156}\text{Dy})]$ overestimates the experimental pairing gaps [37] in these spherical nuclei. The strength optimized only for the spherical nuclei is $V_{\text{opt}}(\text{sph}) = -308.0$ MeV fm $^{-3}$. This

is 10.4 % weaker than $V_{\text{opt}}(\text{def})$.

It is an open problem to construct the pair-DF which allows us to describe the pairing properties along the chains of semi-magic nuclei at the same quality achieved for deformed region [55, 56, 57]. The authors of Ref. [55] considered that the overestimation in spherical nuclei may be partly attributed to the effect of the particle number fluctuation. They showed that the HFB calculation with the approximate particle number projection using the Lipkin-Nogami method improves the agreement with experiment for spherical nuclei. We do not discuss this point further in detail, and the choice of $V_0[\Delta_n(^{156}\text{Dy})]$ is employed in this work.

The strengths V_0 for other Skyrme parameters are also determined by the same procedure. The σ_{tot} with the choice of $V_0[\Delta_n(^{156}\text{Dy})]$ is almost the same quality compared to SLy4 (see Table III). In Fig. 17, the $\Delta_n/\Delta_n^{(A)}$ of Sn and Pb isotopes and the $\Delta_p/\Delta_p^{(A)}$ of $N = 50$ and 82 isotones obtained with Skyrme BSk17, LNS and SkM* are shown. The η_1 and $V_0[\Delta_n(^{156}\text{Dy})]$ in Table III are used for the Skyrme forces. For comparison, the value obtained with the SLy4 force is subtracted; $\delta(\Delta_\tau/\Delta_\tau^{(A)})(X) = \Delta_\tau/\Delta_\tau^{(A)}(X) - \Delta_\tau/\Delta_\tau^{(A)}(\text{SLy4})$ for $X = \text{BSk17, LNS and SkM}^*$. Their $(\Delta m_1, m_v^*/m)$ are $(0.190, 0.800)$, $(-0.028, 0.780)$, $(-0.164, 0.727)$, and $(-0.262, 0.653)$ for SLy4, BSk17, LNS, and SkM* respectively. The σ_{tot} of the BSk17 is smallest, and the κ of SkM* is largest in this work. The LNS parametrization was built to match the I dependence of the effective masses and the neutron matter EOS predicted by Brückner-Hartree-Fock calculation.

In spite of the variety of Δm_1 and m_v^* , the $\delta(\Delta_\tau/\Delta_\tau^{(A)})$ is small along the isotopic and isotonic chains, except for around the subshell closure; $N = 90$ for Δ_n , and $Z = 38$ and 40 for Δ_p . This is because the pairing correlations are sensitive to the single-particle structure around the subshell closure.

The small $\delta(\Delta_n/\Delta_n^{(A)})$ can be expected due to the weak sensitivity of σ_n to η_1 if the strength V_0 is constrained by $\Delta_n^{(\text{exp})}$ of a specific nucleus [24]. This is seen in Fig. 6. Authors of Ref. [58] also pointed out that the Δ_n of Sn and Pb isotope chains are insensitive to Δm_1 by performing the HFB calculation with the mixed type pairing force and various Skyrme forces. On the other hand, the fine tuning of η_1 is indispensable for the small $\delta(\Delta_p/\Delta_p^{(A)})$ due to the sensitivity of σ_p to η_1 . This is shown in Fig. 6, and discussed in Ref. [24].

The $\eta_2 = 2.5$ for SLy4 is commonly used for other Skyrme parameters (see Sec. VI). This is an approximation in our analysis. However, the small $\delta(\Delta_\tau/\Delta_\tau^{(A)})$ as a function α means that the difference in the α dependence of the pairing gaps due to the different Skyrme forces can be small with the fixed $\eta_2 = 2.5$.

We refer the pair-DF with the parameters in Table III as the optimal one for each Skyrme parameterization. The optimal pair-DF with ρ_1 dependence is constructed aiming at unique description of pairing properties toward

the neutron drip line. Our prescription is based on the phenomenological considerations. In this sense, our conclusion is tentative. However, the optimal pair-DF can preserve the good descriptive power of the neutron excess dependence of pairing correlations, and provide the certain foundation for the further improvement with experimental data of nuclei with larger neutron excess.

VIII. CONCLUSION

We proposed a new pair-DF by introducing the ρ_1 dependence. We emphasized the necessity of both the linear and quadratic ρ_1 terms in the pair-DF for the global description of pairing correlations; namely the dependence on both the mass number A and the neutron excess $\alpha = (N - Z)/A$.

To optimize the parameters in the pair-DF, we performed the HFB calculation for 156 nuclei of $A = 118 - 196$ and $\alpha < 0.25$. By the extensive investigation with 13 Skyrme parameterizations, we clarify that the pair-DF should include the ρ_1 dependence in order to take into account the effect of the m_s^* and m_v^* in the p-h channel: The η_1 and m/m_v^* is linearly dependent, and the pairing strength V_0 linearly increases as a function of m_s^*/m with the optimal set of (η_0, η_1, η_2) . The relationship between the optimal η_1 and the splitting of the neutron and proton effective masses is also discussed. The V_0 is fixed so as reproduce the $\Delta_n^{(\text{exp})}$ of ^{156}Dy . With this choice, we can obtain the almost minimum value of the total r.m.s. deviation between the experimental and calculated pairing gaps. The different Skyrme forces with the optimal pair-DF can give the small difference in the pairing gaps toward the neutron drip line.

In this paper, we concentrated on the analysis of pair-

ing gaps in finite nuclei based on the phenomenological consideration. To obtain the deeper insight to the ρ_1 terms in the pair-DF, it is interesting to investigate pairing correlations in asymmetric nuclear matter by comparing the up-to-date calculations with 3-body force and correlations beyond the mean-field approximation. This analysis is a future subject.

Acknowledgments

This work is supported in part by the JSPS Core-to-Core Program, International Research Network for Exotic Femto Systems (EFES) and by Grant-in-Aid for Scientific Research on Innovative Areas (No. 20105003) and by the Grant-in-Aid for Scientific Research (B) (No. 21340073). We are grateful to H. Sagawa, K. Yabana, and K. Matsuyanagi for valuable discussions. The numerical calculations were carried out on Altix3700 BX2 and SX8 at YITP in Kyoto University and the RIKEN Super Combined Cluster (RSCC) in RIKEN.

APPENDIX A: CORRELATION ANALYSIS

We introduce the correlation coefficient r for a data set $(x, y) = \{(x_i, y_i)\}$ ($i = 1, 2, \dots, n$). It is defined by

$$r = \frac{\sum_{i=1}^n (x_i - \bar{x})(y_i - \bar{y})}{\sqrt{\sum_{i=1}^n (x_i - \bar{x})^2} \sqrt{\sum_{i=1}^n (y_i - \bar{y})^2}}. \quad (\text{A1})$$

The coefficient r can take a real value of $-1 \leq r \leq 1$. In the limit of $r = 1$ or -1 , the data set is linearly dependent. On the other hand, the correlation between x and y is weak if r is close to zero.

-
- [1] M. Bender, P.-H. Heenen, and P.-G. Reinhard, *Rev. Mod. Phys.* **75**, 121 (2003).
- [2] D. Vautherin, and D. M. Brink, *Phys. Rev. C* **5**, 626 (1972).
- [3] H. Krivine, J. Treiner, and O. Bohigas, *Nucl. Phys.* **A336**, 155 (1980).
- [4] Nguyen Van Giai and H. Sagawa, *Phys. Lett.* **106B**, 379 (1981).
- [5] J. Bartel, P. Quentin, M. Brack, C. Guet, H.-B. Hakansson, *Nucl. Phys.* **A386**, 79 (1982).
- [6] P.-G. Reinhard, and H. Flocard, *Nucl. Phys.* **A584**, 467 (1995).
- [7] E. Chabanat, P. Bonche, P. Haensel, J. Meyer, and R. Schaeffer, *Nucl. Phys.* **A635**, 231 (1998); Erratum *Nucl. Phys.* **A643**, 441 (1998).
- [8] T. Lesinski, M. Bender, K. Bennaceur, T. Duguet, and J. Meyer, *Phys. Rev. C* **76**, 014312 (2007).
- [9] J. Dobaczewski, W. Nazarewicz, T. R. Werner, J. F. Berger, C. R. Chinn, and J. Dechargé, *Phys. Rev. C* **53**, 2809 (1996).
- [10] D. M. Brink and R. A. Broglia, *Nuclear Superfluidity* (Cambridge University Press, Cambridge, 2005).
- [11] F. Barranco, R. A. Broglia, G. Gori, E. Vigezzi, P. F. Bortignon, and J. Terasaki, *Phys. Rev. Lett.* **83**, 2147 (1999).
- [12] J. Terasaki, F. Barranco, R. A. Broglia, E. Vigezzi, and P. F. Bortignon, *Nucl. Phys.* **A697**, 127 (2002).
- [13] Z. Bochnacki, I. M. Holban, and I. N. Mikhailov, *Nucl. Phys.* **A97**, 33 (1967).
- [14] R. R. Chasman, *Phys. Rev. C* **14**, (1976).
- [15] S. G. Kadenskii, Yu. L. Ratis, K. S. Rybak, and V. I. Furman, *Sov. J. Nucl. Phys.* **27**, 481 (1979).
- [16] G. F. Bertsch, and H. Esbensen, *Ann. Phys. (New York)* **209**, 327 (1991).
- [17] J. Terasaki, P. -H. Heenen, P. Bonche, J. Dobaczewski, and H. Flocard, *Nucl. Phys.* **A593**, 1 (1995).
- [18] J. Dobaczewski and W. Nazarewicz, *Prog. Theor. Phys. Suppl.* **146**, 70 (2002).
- [19] J. Dobaczewski, H. Flocard, and J. Treiner, *Nucl. Phys.* **A422**, 103 (1984).
- [20] K. Bennaceur, J. Dobaczewski, and M. Ploszajczak, *Phys. Rev. C* **60**, 034308 (1999).

- [21] M. Matsuo, K. Mizuyama, and Y. Serizawa, Phys. Rev. C **71**, 064326 (2005).
- [22] M. Yamagami, Phys. Rev. C **72**, 064308 (2005).
- [23] M. Matsuo, Phys. Rev. C **73**, 044309 (2006).
- [24] M. Yamagami and Y. R. Shimizu, Phys. Rev. C **77**, 064319 (2008).
- [25] J. Margueron, H. Sagawa, and K. Hagino, Phys. Rev. C **76**, 064316 (2007).
- [26] J. Margueron, H. Sagawa, and K. Hagino, Phys. Rev. C **77**, 054309 (2008).
- [27] D. J. Dean and M. Hjorth-Jensen, Rev. Mod. Phys. **75**, 607 (2003).
- [28] F. Barranco, P. F. Bortignon, R. A. Broglia, G. Colo, P. Schuck, E. Vigezzi, and X. Vinas, Phys. Rev. C **72**, 054314 (2005).
- [29] A. Pastore, F. Barranco, R. A. Broglia, and E. Vigezzi, Phys. Rev. C **78**, 024315 (2008).
- [30] T. Duguet, Phys. Rev. C **69**, 054317 (2004).
- [31] T. Duguet and T. Lesinski, Eur. Phys. J. Special Topics **156**, 207 (2008).
- [32] A. Fabrocini, S. Fantoni, A. Yu. Illarionov, and K. E. Schmidt, Nucl. Phys. **A803**, 137 (2008).
- [33] S. Gandolfi, A. Yu. Illarionov, S. Fantoni, F. Pederiva, K. E. Schmidt, Phys. Rev. Lett. **101**, 132501 (2008).
- [34] A. Gezerlis and J. Carlson, Phys. Rev. C **77**, 032801 (2008).
- [35] L. G. Cao, U. Lombardo, and P. Schuck, Phys. Rev. C **74**, 064301 (2006).
- [36] P. Vogel, B. Jonson, and P. G. Hansen, Phys. Lett. **139B**, 227 (1984).
- [37] G. Audi, A. H. Wapstra, and C. Thibault, Nucl. Phys. **A729**, 337 (2003).
- [38] M. Anguiano, J. L. Egido, and L. M. Robledo, Nucl. Phys. **A683**, 227 (2001).
- [39] T. Lesinski, T. Duguet, K. Bennaceur, and J. Meyer, Eur. Phys. Jour. A **40**, 121 (2009).
- [40] M. V. Stoitsov, J. Dobaczewski, W. Nazarewicz, and P. Ring, Comput. Phys. Commun. **167**, 43 (2005).
- [41] M. Bender, K. Rutz, P.-G. Reinhard, and J.A. Maruhn, Eur. Phys. J. A **8**, 59 (2000).
- [42] M. Yamagami, K. Matsuyanagi, and M. Matsuo, Nucl. Phys. **A693**, 579 (2001).
- [43] M. Matsuo, Nucl. Phys. **A696**, 371 (2001).
- [44] R. M. Ronningen, R. B. Piercey, J. H. Hamilton, C. F. Maguire, A. V. Ramayya, H. Kawakami, B. van Nooijen, R. S. Grantham, W. K. Dagenhart, and L. L. Riedinger, Phys. Rev. C **16**, 2218 (1977).
- [45] P. Ring and P. Schuck, *The Nuclear Many-Body Problem* (Springer-Verlag, Berlin, 1980).
- [46] M. V. Stoitsov, J. Dobaczewski, W. Nazarewicz, S. Pittel, and D. J. Dean, Phys. Rev. C **68**, 054312 (2003).
- [47] L.G.Cao, U.Lombardo, C.W.Shen, and Nguyen Van Giai, Phys. Rev. C **73**, 014313 (2006).
- [48] S. Goriely, N. Chamel, and J. M. Pearson, Phys. Rev. Lett. **102**, 152503 (2009).
- [49] F. Tondeur, M. Brack, M. Farine, and J. M. Pearson, Nucl. Phys. **A420**, 297 (1984).
- [50] P. -G. Reinhard, D. J. Dean, W. Nazarewicz, J. Dobaczewski, J. A. Maruhn, and M. R. Strayer, Phys. Rev. C **60**, 014316 (1999).
- [51] O. Bohigas, A. M. Lane, and J. Martorell. Phys. Rep. **51**, 267 (1979).
- [52] M. Bender, J. Dobaczewski, J. Engel, and W. Nazarewicz, Phys. Rev. C **65**, 054322 (2002).
- [53] A. Blazkiewicz, V. E. Oberacker, A. S. Umar, and M. V. Stoitsov, Phys. Rev. C **71**, 054321 (2005).
- [54] M. V. Stoitsov, J. Dobaczewski, P. Ring, and S. Pittel, Phys. Rev. C **61**, 034311 (2000).
- [55] G. F. Bertsch, C. A. Bertulani, W. Nazarewicz, N. Schunck, and M. V. Stoitsov, Phys. Rev. C **79**, 034306 (2009).
- [56] C. A. Bertulani, H. F. Lu, and H. Sagawa, Phys. Rev. C **80**, 027303 (2009).
- [57] T. Duguet, P. Bonche, P. -H. Heenen, and J. Meyer, Phys. Rev. C **65**, 014310 (2002); *ibid.* 014311 (2002).
- [58] T. Lesinski, K. Bennaceur, T. Duguet, and J. Meyer, Phys. Rev. C **74**, 044315 (2006).